Research article

Journal of MASS SPECTROMETRY

Received: 2 June 2013 Revised: 30 September 2013 Accepted: 2 October 2013 Published online in Wiley Online Library

(wileyonlinelibrary.com) DOI 10.1002/jms.3293

Quadrupole mass filter operation under the influence of magnetic field

S. U. A. H. Syed, S. Maher and S. Taylor*

This work demonstrates resolution enhancement of a quadrupole mass filter (QMF) under the influence of a static magnetic field. Generally, QMF resolution can be improved by increasing the number of rf cycles an ion experiences when passing through the mass filter. In order to improve the resolution, the dimensions of the QMF or the operating parameters need to be changed. However, geometric modifications to improve performance increase the manufacturing cost and usually the size of the instrument. By applying a magnetic field, a low-cost, small footprint instrument with reduced power requirements can be realized.

Significant improvement in QMF resolution was observed experimentally for certain magnetic field conditions, and these have been explained in terms of our theoretical model developed at the University of Liverpool. This model is capable of accurate simulation of spectra allowing the user to specify different values of mass spectrometer dimensions and applied input signals. The model predicts enhanced instrument resolution $R>26\,000$ for a CO_2 and N_2 mixture with a 200-mm long mass filter operating in stability zone 3 via application of an axial magnetic field. Copyright © 2013 John Wiley & Sons, Ltd.

Keywords: quadrupole mass filter (QMF); resolution; magnetic field; U/V ratio; ion trajectories

Introduction

First constructed by J. J. Thomson in 1913, a mass spectrometer (MS), then called a parabola spectrograph,[1] was used to separate ions by their different parabolic trajectories in electromagnetic fields. Ions were detected upon striking a fluorescent screen or photographic plate.

Later, Thomson's protégé, Francis W. Aston designed an MS with resolution improved by an order of magnitude, allowing applications to isotopic analysis.[2] At the same time, A. J. Dempster also improved the resolution with a magnetic analyzer and developed the first electron impact source, which ionizes volatilized molecules with a beam of electrons.[3] Thomson, Aston and Dempster provided a strong foundation for MS instrument design and theory for those who followed to develop instruments capable of meeting the demands of analytical chemists and biologists. An important issue, particularly for chemists, was the need of an instrument with improved accuracy for the analysis of elements and small organic molecules.[4] This led to the development of four different types of MS instrument: magnetic sector double focusing,[5] time-of-flight,[6] quadrupole[7] and Fourier transform ion cyclotron resonance[8] mass analyzers.

The use of an electrodynamic quadrupole field for mass spectrometry dates back to the pioneering work of Wolfgang Paul and co-workers in the 1950s.[9] It is widely used as a mass filter in a quadrupole mass spectrometer (QMS) instrument, or as an ion guide or as a linear ion trap.[10] Since then, much research has been undertaken by different researchers to study the performance and behavior of the QMS by either experimental methods or by numerical simulation techniques. In 1962, Von Zahn, a member of the Paul group, constructed a mass filter of 5.82 m in length with a reported resolution in the region of 16 000 (measured at 50% peak width definition) for high-precision mass measurements.[11] Later, Brubaker and Tull investigated the transmission efficiency and resolution of a QMF as a function of ion source exit aperture and frequency of excitation; the ion source exit aperture defines the area of illumination of the QMF and is usually a fraction of the inscribed QMF field radius (r_0).[12] It was concluded that higher resolution is obtained with small aperture size and higher frequency. In 1971, Holme *et al*. performed a series of experiments to investigate the factors which determine the maximum resolution of a QMS under normal operating conditions and it was found that the resolution depends upon the number N of radio frequency (rf) cycles the ion experiences in the quadrupole field.[13] In Dawson (1976), the design and performance of the QMF are described in detail, and it was reported that resolution R can be represented by $\boldsymbol{R = N^n/K}$, where n is either exactly or closely equal to 2, and K is a constant which may be assumed to be 20 for all practical purposes [14, chapter 6]. N further depends upon frequency (f) of the rf signal, length (l) of the mass filter, ion injection energy (E_z) and mass (m) of the ion.

There have been many analytical predictions of the behavior of QMS. In 1987, Batey presented a detailed review of quadrupole gas analyzers and showed that some features of the behavior of the QMS could be predicted by tracing the ion motion through the mass filter.[15] Later, in 1993, Konenkov investigated the influence of fringing fields on the acceptance of a QMF in the separation mode of the intermediate stability region.[16] Other workers presented a numerical method which can be adequately used for mass independent optimization of the performance of quadrupole pre-filters.[17] It was reported that in the numerical method neither the effects of fringe fields nor those of initial transverse velocities

* *Correspondence to: Stephen Taylor, Department of Electrical Engineering and Electronics, University of Liverpool, Brownlow Hill, Liverpool, L69 3GJ, UK. E-mail: s.taylor@liv.ac.uk*

Department of Electrical Engineering and Electronics, University of Liverpool, LiverpoolL69 3GJ, UK

were taken into consideration; however, there was good agreement with the measured transmission data obtained. Muntean used matrix methods to develop a computer simulation program to model ion transmission through the filter by calculating ion trajectories in rf only quadrupoles.[18] Tunstall *et al*. described the development of a computer program designed to simulate the performance of the mass filter in an ideal QMS.[19] Their simulation program provided flexible input parameters to allow the user to investigate the ion trajectories and transmission efficiency for different operating conditions.

Gibson and Taylor have also developed computational methods to determine the trajectories of a large number of ions injected into the QMS, providing a detailed computer simulation for both hyperbolic and circular cross-section electrodes.[20,21] Du *et al*. theoretically modeled peak structures for a QMF operating in zone 3[22]; it was suggested that to improve the peak structures, changes in ion inlet optics or changes to ion detection geometry were required. Douglas *et al*. examined the effect of displacement of QMF electrodes with circular electrodes on spatial harmonics, and it was concluded that the data can be useful in designing quadrupole mass filters (QMFs).[23] Other workers performed simulations to determine the required resolution for the qualitative and quantitative identification of low mass isotopes in the mass range 1–6 amu.[24] More recently, Ahn and Park simulated electron and ion trajectories for an electron-impact ion source coupled to a QMS. It was shown that computer simulation of electron and ion trajectories can be utilized for the characterization and optimization of the electron-impact ion source.[25]

Magnetic fields have long been used in quadrupole ion sources, magnetic sector instruments[26] and in ion traps[27] to increase the performance or the resolution. However, surprisingly little work has been done in relation to the application of magnetic field to the QMF. Previously published experimental and theoretical results for QMF operating in stability zone 1 showed: the effect of a transverse magnetic field on the resolution of QMF,[28] the effect of a static magnetic field on the ion trajectories[29] and the effect of an axial magnetic field on the performance of a QMF.[30] For QMF operating in stability zone 3, previous work had shown the effect of transverse magnetic field on resolution.[31] In this paper, therefore, we present new experimental and simulation results explaining the performance of QMF operating in stability zones 1 and 3 under the influence of magnetic field in detail. The results presented provide useful information for the design of novel quadrupole instruments and/or using an existing QMF with applied magnetic field for new applications.

Theory of a QMF under the influence of magnetic field

The force *F*, exerted on an ion with charge *q*, moving with velocity *v*, through an electric field *E*, and magnetic field *B*, is given by the Lorentz force, $\boldsymbol{F} = q\,(\boldsymbol{E} + \boldsymbol{v} \times \boldsymbol{B})$.[32] If the electric field is given by conventional quadrupolar potential where *U* is the amplitude of dc potential applied to electrodes, *V* the amplitude of rf potential, *f* the frequency of the sinusoidal field and r_0 the inscribed radius of the electrodes, for a general field $\boldsymbol{B} = (B_x, B_y, B_z)$, the coupled equations of motion are given by:

$$\frac{d^2x}{d\xi^2} = -x\,(a - 2qcos2\xi) + \left(\frac{dy}{d\xi}b_3 - \frac{dz}{d\xi}b_2\right) \quad (1)$$

$$\frac{d^2y}{d\xi^2} = y(a - 2qcos2\xi) + \left(\frac{dz}{d\xi}b_1 - \frac{dx}{d\xi}b_3\right) \quad (2)$$

$$\frac{d^2z}{d\xi^2} = \left(\frac{dx}{d\xi}b_2 - \frac{dy}{d\xi}b_1\right). \quad (3)$$

In the numerical model, the above equations have been written in a dimensionless form where the only dimension that appears is that of length displacement. The time *t* has become $t = 2\xi/\omega$ where ω is the angular frequency equal to $2\pi f$. In the absence of an applied magnetic field, the direct potential *U* and alternating potential *V* are related to *a* and *q* as

$$a = \left(\frac{4eU}{mr_0^2\omega^2}\right) \quad (4)$$

$$q = \left(\frac{2eV}{mr_0^2\omega^2}\right) \quad (5)$$

The components of the ***B*** field are:

$$(b_1, b_2, b_3) = \left(\frac{2eB_x}{m\omega}, \frac{2eB_y}{m\omega}, \frac{2eB_z}{m\omega}\right). \quad (6)$$

In this study, we assume that the QMF electrodes in the *x-z* plane are supplied with a positive potential and the pair of electrodes in the *y-z* plane are supplied with a negative potential. The static magnetic field is projected either axially (along the *z* plane) or transversely (along the *x-z* plane or the *y-z* plane). For the transverse case, applying the magnetic field along the *x*-axis is equivalent to applying the magnetic field along the *y*-axis only with the electrode potentials reversed and the stability zone quadrant of operation switched.[33] It can be seen from Eqns (1 – 3) that if the magnetic field is taken to be zero the coupled differential equations reduce to the familiar Mathieu equations for a linear quadrupole. Solving numerically, the coupled differential equations give the trajectories of the ions through the mass filter. From the trajectories, it is feasible to determine the conditions which give successful ion transmission for a given mass to charge ratio. This depends on the values of direct potential *U*, the rf potential *V*, the rf voltage frequency *f*, the inscribed radius of the quadrupole electrodes r_0, the magnetic field ***B***, the initial velocity, initial phase and the ion position. The first four parameters appear as the variables of *a* and *q* in the Mathieu equation for ($B = 0$).

For ***B*** non-zero, there will be a further dependence of ion stability upon the magnetic field and this dependency is shown for one specific case (*Bx*) in Fig. 1. The magnetic field vector applied transversely along the *x*-axis causes the stability region to become narrower for the ***y* stability boundary** (Fig. 1). Increasing the *x*-magnetic field for given operating conditions leads to a reduction in the **low mass side** of the mass spectra resulting in reduced peak width. Moreover, it can be seen from the figure that upon application of ***Bx*** the tip of the stability diagram changes according to its intensity thus changing the ideal

Journal of MASS SPECTROMETRY

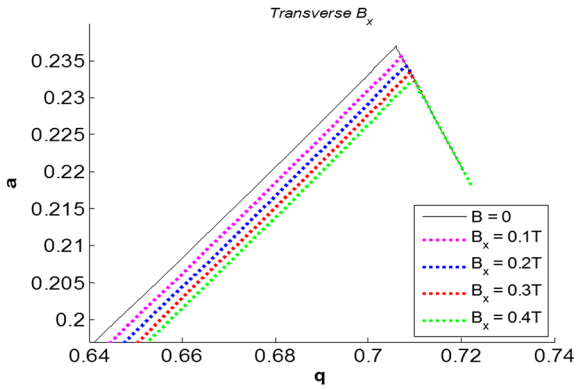

Figure 1. Mapped Zone 1 Stability Tip for various B_x.

operating point (*U/V*) ratio for a scan line. A complete analysis for mapping the stability diagram with an applied magnetic field has been published recently.[33]

Software

A custom software program (QMS-hyperbolic) developed in Visual C++ environment is used. The program calculates ion trajectories by solving the Mathieu equations using a fourth-order Runge–Kutta algorithm. It operates by dividing the ion trajectories into small time steps and assuming that over the steps the ion motion in three directions *x*, *y* and *z* is uncoupled. Mass scans are computed by ramping the values of *U* and *V* with fixed *U/V* ratio, which sets the resolution of an instrument. An option of introducing magnetic in all the three directions (B_x, B_y, B_z), along the whole length of the mass filter, is also incorporated. The original model[30,31] has been upgraded to provide: improved sensitivity (using a larger number of steps along the mass scale), to include large number of ions at each point on the mass scale and to simulate a QMF with a very large number of rf cycles.

A second program (IonSrc) allows entry conditions for large number of ions (typically 10^8), to be specified, which are subsequently supplied to the mass filter calculation engine to simulate individual trajectories in each case. The IonSrc program assumes a uniformly illuminated ion distribution across a user-defined ion source exit radius. Each ion is injected into the QMF with random phase with respect to the rf at the time of entry. Finally, Matlab and Microsoft Excel were used to post process the data and for the generation of graphical results. From the mass spectra obtained experimentally or by numerical simulation, the resolution *R* was found by using the equation $R = M/\Delta M$,[14] where *M* is the mass of the given spectral peak and ΔM is the width of the mass peak measured at 10% of its height.

QMF in the first stability zone with magnetic field applied

Effect of transverse magnetic field on the performance of a QMF operating in zone 1

Experimental results

Reported here are the experimental mass peaks for $^4He^+$, $^{40}Ar^+$ and Xe^+ ions with and without a transverse magnetic field. A conventional single filter QMS instrument supplied by MKS Spectra Products (Crewe, UK) was used. The QMF length was 100 mm with an electrode diameter of 6.35 mm and field radius of 2.76 mm, excited at 1.8342 MHz. The instrument was operated in Faraday only mode and in this configuration is typically used as a Residual Gas Analyzer (RGA). The QMS was housed in a stainless steel vacuum chamber pumped by a turbo pump, backed by a diaphragm pump providing a residual gas pressure of 7×10^{-7} torr. After admitting the sample gas into the vacuum chamber, the working pressure was raised to about 2×10^{-5} torr. The transverse magnetic field was applied through the use of bar magnets fixed on a steel yoke around the mass filter. For the experiments mentioned, the magnetic field was increased by reducing the distance between the bar magnets and was measured using a Hall Effect sensor. The ion energy was set at 5 eV; this gives an appreciable ion current signal. The emission current was set to 0.3 mA and the electron energy in the QMS ion source was set at 70 eV. The magnetic field extended 70% of the length of QMF. To demonstrate the effect of magnetic field in the *x* direction on resolution of the QMF, $^4He^+$, $^{40}Ar^+$ and Xe^+, mass peaks were obtained with and without the magnetic field B_x applied.

Effect of Bx on $^4He^+$

Figure 2a shows typical mass peaks obtained experimentally from the QMS for $^4He^+$ with and without magnetic field. As

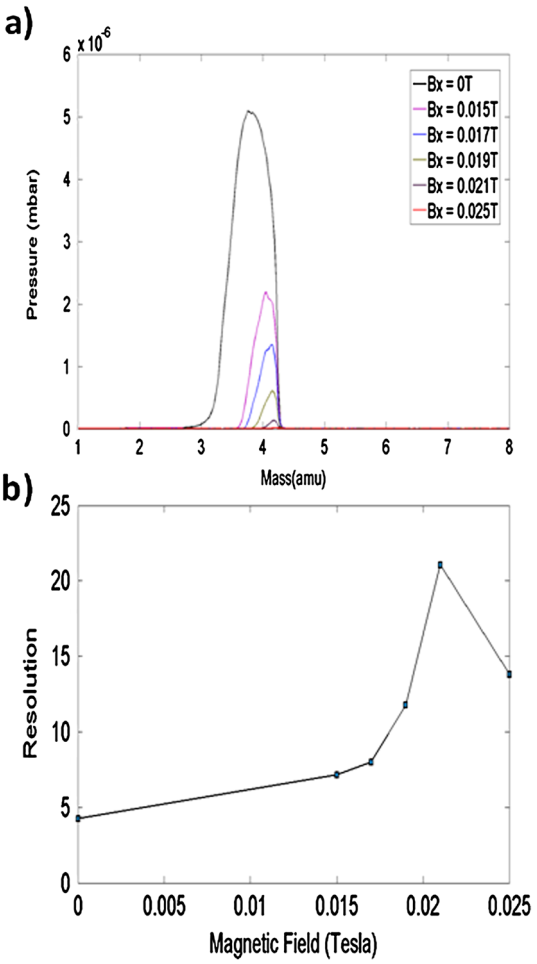

Figure 2. (a) Mass peaks obtained experimentally from the QMS for $^4He^+$ with and without magnetic field; (b) Behavior of the resolution of $^4He^+$ as a function of transverse magnetic field.

seen from Fig. 2a, an increase in resolution (defined as $R = M/\Delta M$ at 10% peak height) is clearly observed upon application of magnetic field. The resolution improvement arises from a reduction in peak width with applied magnetic field which occurs on the low-mass tail of the mass spectra. Figure 2b shows the behavior of the resolution as a function of transverse magnetic field. The resolution increases by up to a factor of 5 as *Bx* is varied between 0 and 0.021 T (approximately from R = 4 to R = 21), and then decreases as it is varied between 0.021 and 0.025 T, indicating that the QMF resolution will not increase indefinitely with *Bx*. This is because as *Bx* increases, the peak shape eventually degrades because of decrease in sensitivity (peak height).

Effect of Bx on $^{40}Ar^+$

Figure 3a shows typical mass peaks obtained experimentally from the QMS for $^{40}Ar^+$ with and without magnetic field. From Fig. 3a, the following observations are made:

(i) There is an improvement in resolution in all cases in which the magnetic field is applied compared with *Bx* = 0 T. However, for the case *Bx* = 0.015 T, there is an increase in both transmission and resolution.

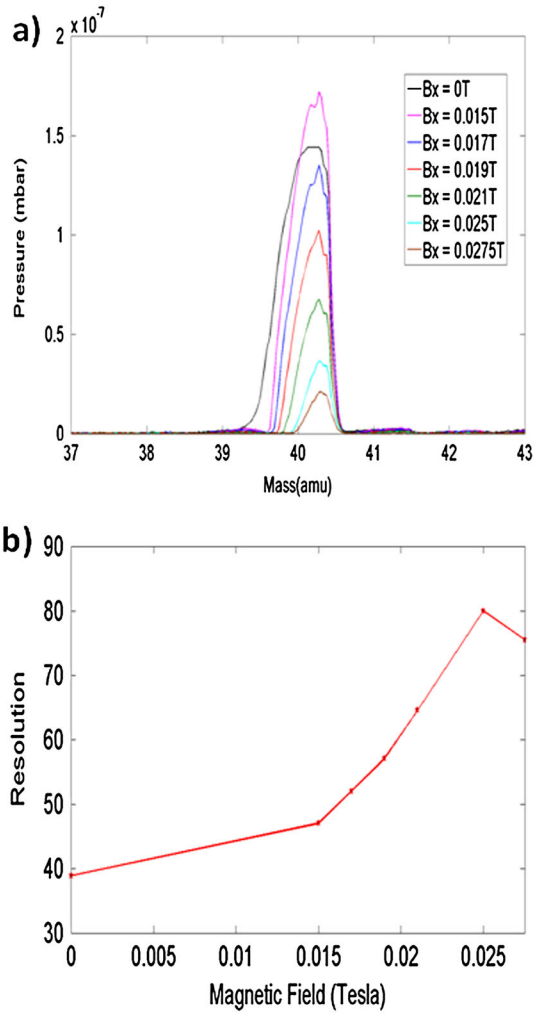

Figure 3. (a) Mass peaks obtained experimentally from the QMS for $^{40}Ar^+$ with and without magnetic field; (b) Behavior of the resolution of $^{40}Ar^+$ as a function of transverse magnetic field.

(ii) For larger values of magnetic field >0.015 T, transmission through the QMF decreases as magnetic field increases.
(iii) The resolution of the mass peak for the case *Bx* = 0.025 T is higher than for the case *Bx* = 0.0275 T.

Possible reasons for these observations are given. Observation (i) could be due to leakage flux from the permanent magnet affecting the ion source. A small amount of leakage flux into the source will cause increased electron path lengths this results in increased ionization and hence increased ion injection into the mass filter for a given electron emission current. A similar kind of effect was observed by Sringengan *et al.*[29] However, for larger magnetic field intensities (observation (ii)), transmission decreases because of the following possible reasons:

(1) At high magnetic field intensities, more electrons remain confined or trapped close to the ionization region. The resulting negative space charge has the effect of impeding electrons from reaching the ionization chamber. The ion source geometry and the magnetic field direction with respect to the QMS head axes can contribute significantly to the onset of this effect to the extent that it causes a reduction in the number of ions injection into the QMF.
(2) Increased Bx intensity leads to increased instability [33] and hence more ions are rejected.
(3) Increased magnetic fields may affect the detector efficiency as fringe fields caused by the magnetic field near the detector cause ions to be lost resulting in reduced sensitivity.

Figure 3b shows the behavior of the resolution as a function of transverse magnetic field for $^{40}Ar^+$ ions. The resolution increases by more than a factor of 2, approximately from *R* = 39 at *Bx* = 0 T to *R* = 100 at *Bx* = 0.025 T, and then decreases as *Bx* is varied between 0.025 and 0.0275 T, since peak shape eventually degrades.

Effect of Bx on Xe^+

Figure 4a shows typical mass peaks obtained experimentally from the QMS for Xe^+ with *Bx* = 0 T, whereas Fig. 4b shows typical mass peaks obtained experimentally for Xe^+ with *Bx* = 0.045 T. Xenon has nine naturally occurring stable isotopes. As seen from Fig. 4a, in the absence of magnetic field, the isotopes of xenon between 128 and 132 *amu* are not completely separable from each other. The application of magnetic field (Fig. 4b) ensures that the minimum resolution required to distinguish the isotopes has been achieved. Although such instrument resolutions are low in comparison with more sophisticated instruments (e.g. triple filter QMFs), this experimental result illustrates the resolution enhancement provided by transversely applied magnetic field.

Simulation results

The effect of U/V ratio on the performance of QMF with applied magnetic field in the x direction

Reported in Fig. 5 are the simulated mass peaks for $^{40}Ar^+$ ions generated using the computer software. All the simulations used 150 steps across the mass range, with 2.5×10^5 ion trajectories simulated at each point. Mass peaks for $^{40}Ar^+$ are generated for a hyperbolic QMF with length (*l*) of 100 mm. The inscribed radius of the QMF was taken to be 2.6 mm. The frequency of the rf voltage used in the simulation was 4 MHz and the ion energy was set at 5 eV. The ion source exit radius (r_{ie}) was set at 0.5 mm.

Journal of MASS SPECTROMETRY

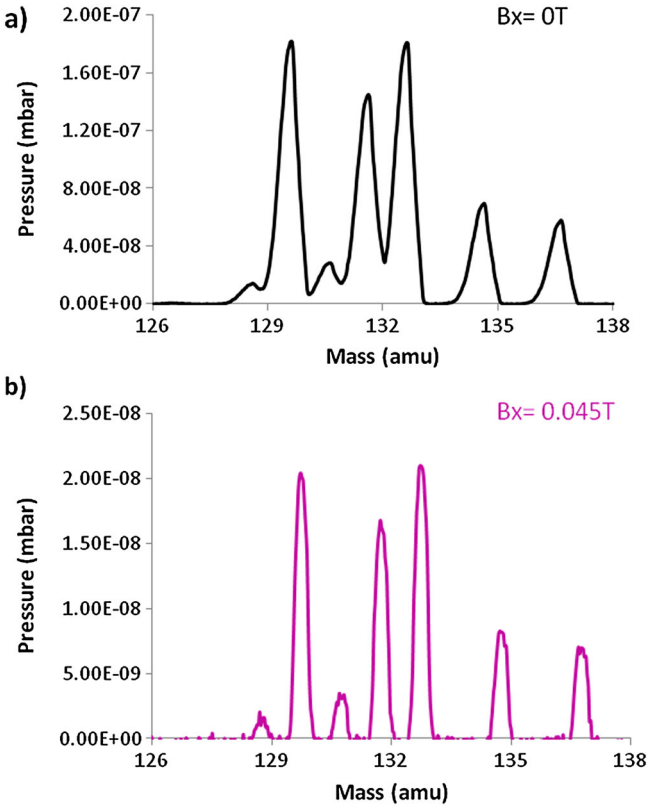

Figure 4. Mass peak for Xe^+ (a) Bx = 0 T; (b) Bx = 0.045 T.

Figure 5a shows the dependency of resolution on *U/V* ratio with and without transverse magnetic field applied in the *x* direction (Bx = 0.02 T). For both the cases, resolution increases with increase in *U/V* ratio; however, the QMF resolution will not increase indefinitely with *U/V* ratio. This is because as *U/V* ratio increases, the peak shape eventually degrades. In the case of magnetic field applied for the selected operating conditions, the resolution peaked at *U/V* = 99.5%, with optimum maximum value of ~445. In the case of no magnetic field applied, the resolution peaked at *U/V* = 99.99%, with a maximum value of ~272. At *U/V* ratio = 99.5% and in the presence of *Bx*, the predicted value of resolution (~445) if achieved in practice is ~64% higher than the resolution (~272) obtained for a QMF operating without magnetic field with the same number of rf cycles at *U/V* ratio near to the apex of Mathieu stability zone 1. This result predicts that for certain values of *U/V* ratio, there is a resolution enhancement upon application of transverse magnetic field.

Figure 5b shows set of peaks for $^{40}Ar^+$ for a hyperbolic QMF at different values of *U/V* ratio with magnetic field applied in the *x* direction (Bx = 0.02 T); whereas, Fig. 5c shows a set of peaks for $^{40}Ar^+$ for a hyperbolic QMF at different values of *U/V* ratio with no magnetic field applied. At the largest value of resolution with magnetic field applied (R = 445, *U/V* = 99.5%), 4500 ions are transmitted at the spectral peak maxima; and at the largest value of resolution with no magnetic field applied (R = 272, *U/V* = 99.99%), 5525 ions are transmitted at the spectral peak maxima. Though there is a loss in transmission of ~19%, resolution is significantly increased by ~64%. Moreover, it is noteworthy that in the presence of magnetic field, the expected value of resolution at *U/V* = 99.3% is ~335 (representing an ~23% increase from the largest value with no *Bx*), and at the spectral peak maxima 23 813 ions are transmitted. An increase in resolution as well as

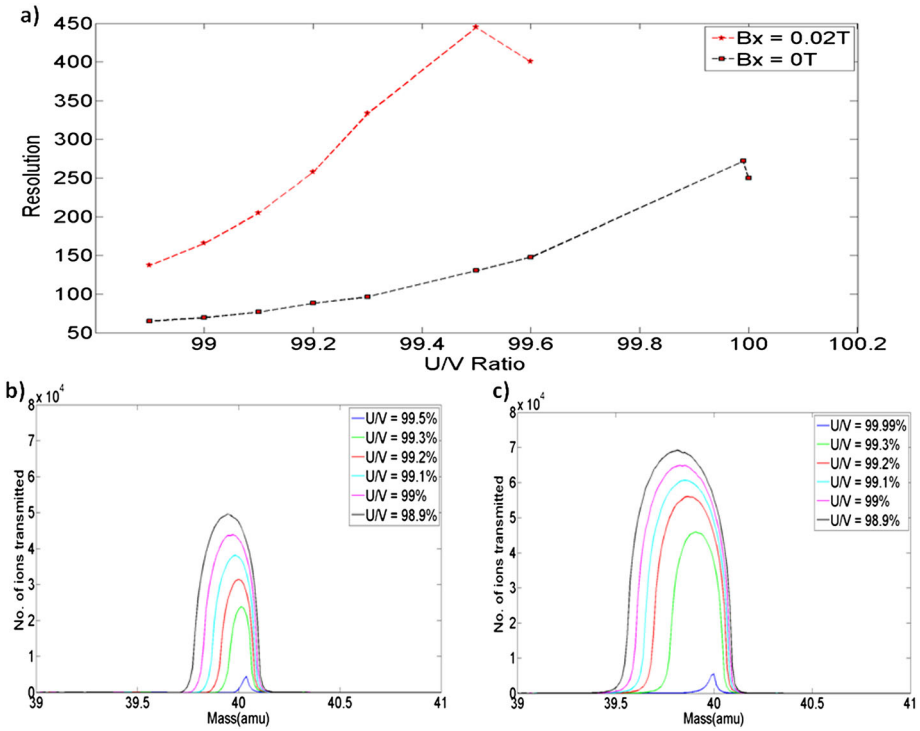

Figure 5. (a) shows the dependency of resolution on *U/V* ratio with and without transverse magnetic field in the *x* direction; (b) set of peaks for $^{40}Ar^+$ within a hyperbolic QMF at different values of *U/V* ratio with magnetic field (Bx = 0.02 T) applied in the *x* direction; (c) set of peaks for $^{40}Ar^+$ within a hyperbolic QMF at different values of *U/V* ratio with no magnetic field applied.

transmission by more than a factor of 4 (5525 to 23 813) is clearly observed in the presence of magnetic field applied if we compare $Bx = 0.02$ T, $U/V = 99.3\%$ with $Bx = 0$ T, $U/V = 99.99\%$. These results are in accordance with[33] where an ultimate increase in resolution of ~75% was predicted when applying a B_x field (against B = 0) for a given set of simulation conditions and for yielding the same percentage transmission for each case.

The effect of magnetic field in the x direction on the resolution of QMF

Figure 6a shows the behavior of the resolution as a function of transverse magnetic field for *U/V* ratio 99.5%, where 100% corresponds to the intersection of the scan line with the apex of the Mathieu stability zone 1. The resolution increases as *Bx* is varied between 0 and 0.02 T, and then decreases. This result is in agreement with our experimental study and shows that for any fixed value of *U/V* ratio (the limit of which depends upon operating conditions) there is a reduction in peak width by simply applying transverse magnetic field to the body of the mass filter.

Figure 6b shows a set of $^{40}Ar^+$ mass spectral peaks for a hyperbolic QMF at different values of magnetic field applied in the *x* direction. Reduction in the low mass tail of the spectra is clearly observed up to a magnetic field of 0.02 T at the expense of reduction in number of ions transmitted.

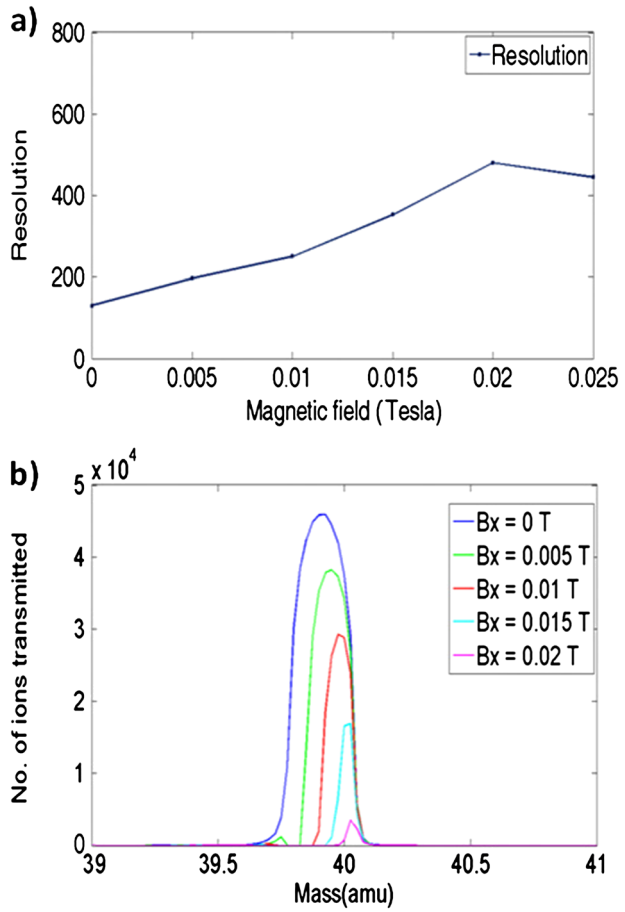

Figure 6. (a) The effect of magnetic field on resolution of $^{40}Ar^+$ applied in the *x* direction for *U/V* 99.5%, (b) simulated mass peaks for $^{40}Ar^+$ with and without magnetic field for *U/V* 99.5%.

Figure 7 shows a set of mass spectral peaks for $^{40}Ar^+$ at different values of magnetic field for *U/V* ratio 99.99%. As seen from Fig. 7, upon application of very small magnetic fields, the mass spectrum suffers from a post cursor peak, degradation in the peak and loss of sensitivity. The ideal operating point is different in the presence of magnetic field in the *x* direction because the tip of the stability diagram alters (Fig. 1). Moreover, the effect of the magnetic field also depends upon the operating parameters of the QMF which are explained in the following sections of this paper.

The effect of magnetic field in the x direction on ion trajectories

Figure 8 shows typical behavior of the ion trajectories calculated using the theoretical model for ions transmitted with and without a transverse magnetic field applied. The corresponding traces shown in the figure are for the same ion injected into the mass filter at the same point in time (rf phase) and space and at the same point on the mass scale (m = 39.91 amu). The upper trace of the figure is for the case with no field applied and lower trace with B_x of 0.02 T.

Ion motion in Fig. 8 originates at $x = 7.77 \times 10^{-5}$ m and $y = 8.7 \times 10^{-5}$ m with an initial velocity of 4.90×10^3 m/s. In the lower trace, due to the additional magnetic field component of the Lorentz force[32] provided by B_x, the amplitude of ion trajectory in *y* direction increases; however, ion trajectory in the *x* direction remains unaffected. The application of magnetic field therefore displaces the ion in the *y* direction so that the ion is lost through impact with the electrodes ($r_0 = 2.6$ mm). It should be noted that ion motion in the *x* direction (parallel to field) is virtually unaffected; it is ion motion in the *y* direction (perpendicular to the field) which is modified.

The effect of frequency on resolution of QMF in the presence of magnetic field in the x direction

Figure 9 shows the effect of frequency on resolution in the presence of a magnetic field. With a transverse magnetic field applied, the effect of frequency of the rf signal on resolution is different to that normally observed for a conventional QMF. The resolution ***decreases*** with increase in frequency and transmission increases. This effect is due to the increased Lorentz force provided in the transverse direction by the magnetic field. Figure 9a shows the dependence of resolution on frequency with an applied magnetic field; whereas, Fig. 9b shows mass peaks for $^{40}Ar^+$ at different frequencies with an applied magnetic field of $Bx = 0.02$ T.

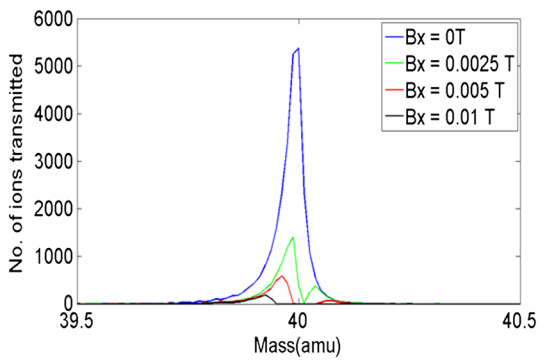

Figure 7. Simulated mass peaks for $^{40}Ar^+$ with and without magnetic field for *U/V* 99.99%.

Journal of MASS SPECTROMETRY

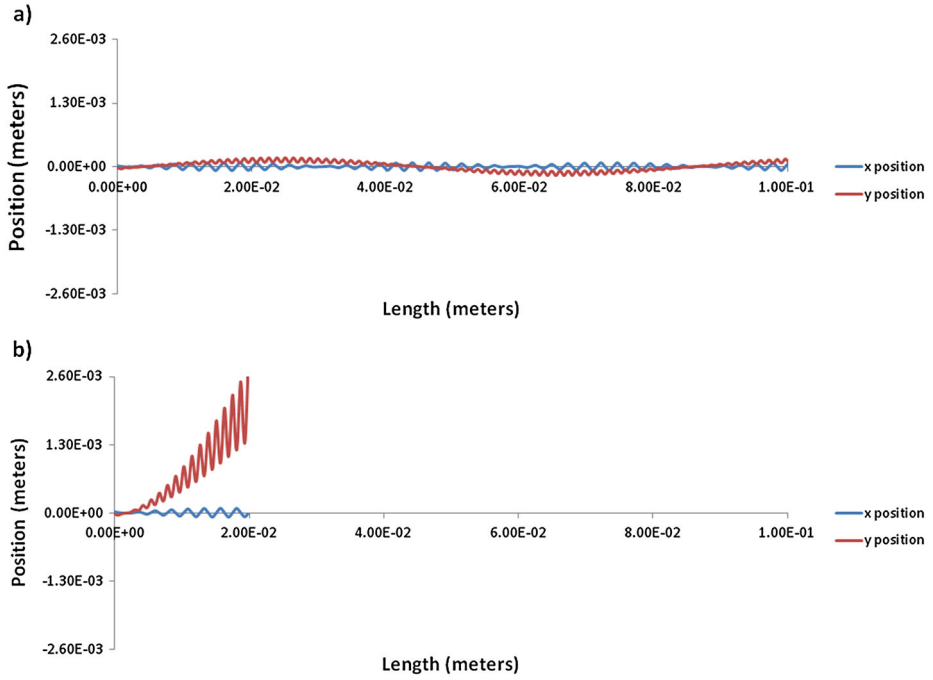

Figure 8. Numerical simulation of ion trajectories in *x* and *y* directions for $^{40}Ar^{+}$ with (a) B_x = 0 T (upper trace) and (b) B_x = 0.02 T (lower trace).

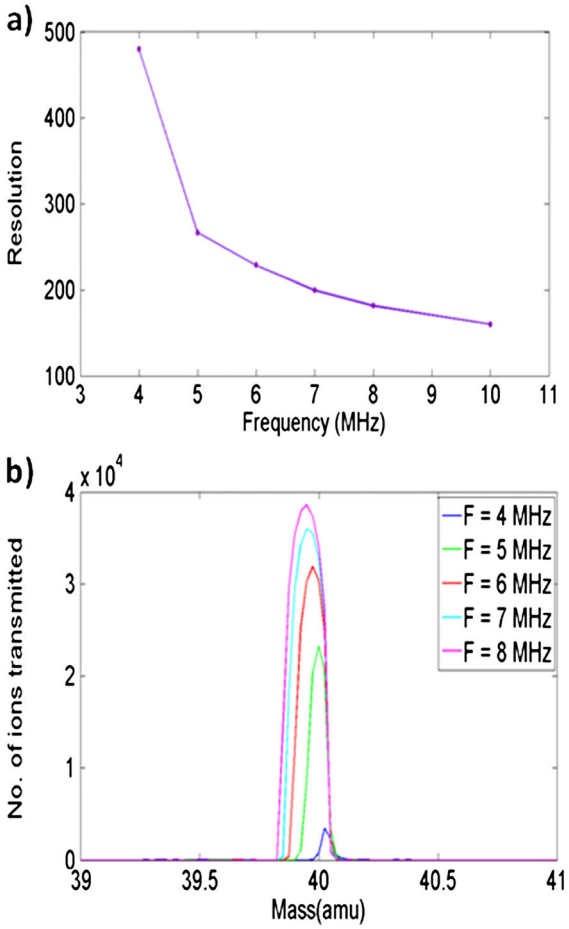

Figure 9. (a) The dependence of resolution on frequency with an applied magnetic field; (b) mass peaks for $^{40}Ar^{+}$ at different frequencies with applied magnetic field of *Bx* = 0.02 T.

The effect can be best demonstrated by examining individual ion trajectories in the presence of a transverse magnetic field at different frequencies of applied rf voltage (V). Figures 8 and 10 show trajectories of ions transmitted with and without magnetic field, at frequencies of 4 and 10 MHz, respectively. The corresponding traces shown in the figures are for the same ion injected into the QMF at the same point in time (rf phase) and space and at the same point on the mass scale (m = 39.91 amu). In both figures, the upper trace is for the case with no field applied and lower trace with B_x of 0.02 T. In Fig. 8, the ion was not transmitted as its position exceeded the field radius.

In Fig. 10, the ion motion also originates at $x = 7.77 \times 10^{-5}$ m and $y = 8.70\times 10^{-5}$ m with the same initial velocity of 4.90×10^{3} m/s. It can be observed from the figure that increase in frequency has a significant impact on behavior of ion trajectories in the presence of magnetic field. It can be seen that ion motion in the *x* direction remains unaffected and the increase in amplitude of ion motion along *y*-axis is less compared to Fig. 8b (less than $r_0 = 2.6$ mm). Therefore, the ion was successfully transmitted in the presence of the magnetic field at the higher frequency of 10 MHz. In this case, although the magnetic field is the same as Fig. 8 (B_x = 0.02 T), the mean ion velocity in the *y* direction increases since the frequency is greater. Therefore, the magnetic component of the Lorentz force experienced by an ion in the *x* direction reduces at higher frequencies since $F = qB_x\sqrt{v_z^2 - v_y^2}$. It can be concluded that for a QMF with magnetic field applied in the *x* direction, the effect of magnetic field on resolution enhancement is more profound at lower frequencies.

The effect of ion energy on resolution of QMS in the presence of magnetic field in the *x* direction

Experimental results

Figure 11 shows the effect of ion energy on resolution in the presence of a magnetic field. With a transverse magnetic field

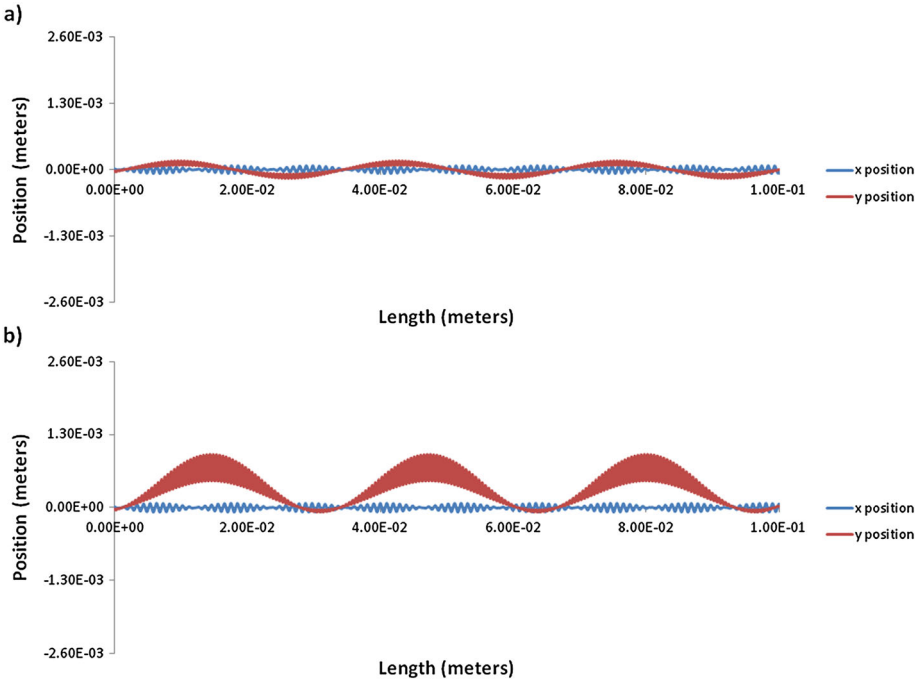

Figure 10. Numerical simulation of ion trajectories in *x* and *y* directions for $^{40}Ar^{+}$ with f = 10 MHz and with (a) B_x = 0 T (upper trace) and (b) B_x = 0.02 T (lower trace).

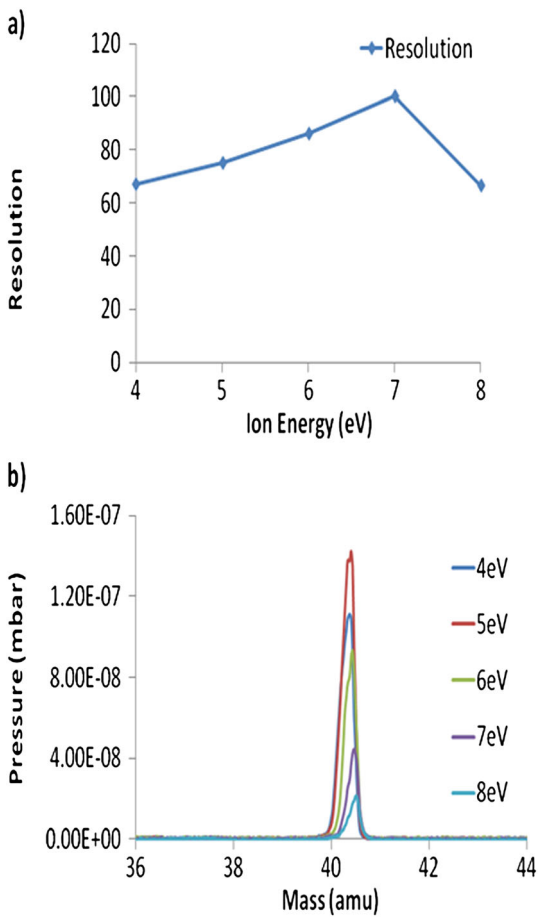

Figure 11. (a) Dependence of resolution on ion energy with an applied magnetic field, measured results; (b) experimental mass peaks for $^{40}Ar^{+}$ at different ion energies with applied magnetic field of Bx = 0.02 T.

applied, the effect of ion energy on resolution is *different* to that normally observed in a conventional QMS. The resolution increases with increase in ion energy from 4 to 7 eV and then decreases. This effect is attributed to the increased Lorentz force experienced by higher energy ions. The minimum ion energy was set at 4 eV to get a measurable signal and then increased in steps of 1 eV. Figure 11a shows the dependence of resolution on ion energy with an applied transverse magnetic field; whereas, Fig. 11b shows measured spectra for $^{40}Ar^{+}$ at different ion energies with applied magnetic field of Bx = 0.02 T.

Simulation results

Figure 12 shows the effect of ion energy on resolution in the presence of a magnetic field via simulations. The trend is similar to that observed experimentally (Fig. 11). The resolution increases with increase in ion energy from 2 to 5 eV and then decreases. Figure 12a shows the dependence of resolution on ion energy with an applied magnetic field; whereas, Fig. 12b shows measured spectra for $^{40}Ar^{+}$ at different ion energies with applied magnetic field of Bx = 0.02 T.

The effect can be evaluated by considering individual ion trajectories in the presence of a transverse magnetic field at different ion energies. Figures 13 and 14 show trajectories of ions transmitted with and without magnetic field, at ion energies of 2 and 5 eV, respectively. The corresponding traces shown in the figures are for the same ion injected into the QMF at the same point in time (rf phase) and space and at the same point on the mass scale (m = 40.00 amu). In both figures, the upper trace is for the case with no field applied and lower trace with B_x of 0.02 T.

Ion motion in Fig. 13 originates at $x = -4.84 \times 10^{-4}$ m and $y = 7.45 \times 10^{-4}$ m with initial velocity of 3.10×10^{3} m/s. It can be seen from the figure that in the presence of magnetic field at lower ion energy (2 eV), ion motion in *y* direction is affected; however, the increase in amplitude of ion trajectory in the *y* direction is not

Journal of MASS SPECTROMETRY

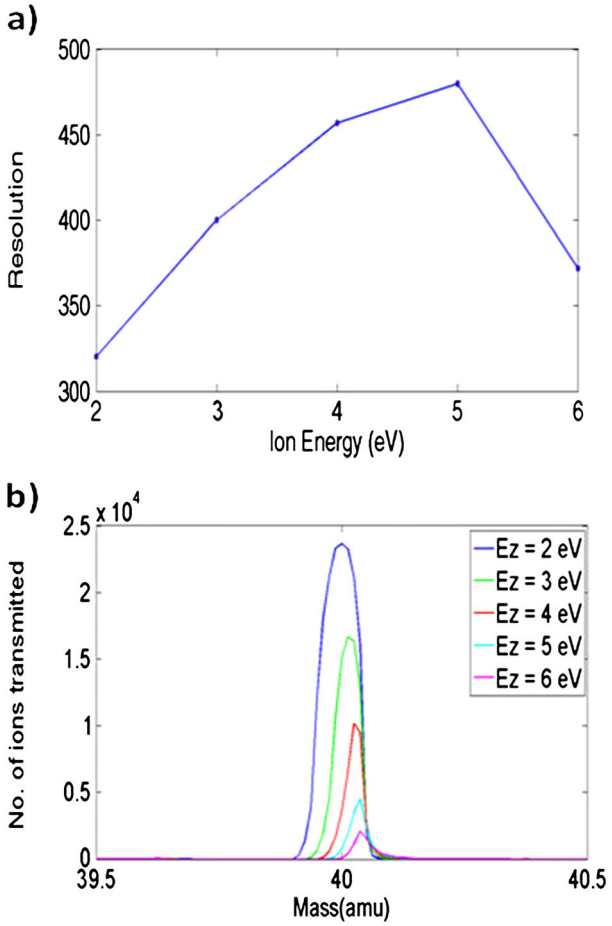

Figure 12. (a) The dependence of resolution on ion energy with an applied magnetic field; (b) simulated mass peaks for $^{40}Ar^{+}$ at different ion energies with applied magnetic field of $Bx = 0.02$ T.

sufficient for the ion to be rejected by exceeding the field radius. In Fig. 14, the ion motion also originates at $x = -3.35 \times 10^{-4}$ m and $y = 1.64\times 10^{-4}$ m with the same initial velocity of 4.90×10^{3} m/s. It can be observed from the figures that increase in ion energy (5 eV) has a major impact on behavior of ion trajectories in the presence of magnetic field. The amplitude of ion trajectory in the y direction increases so far that the ion is lost as the field radius is exceeded. It can be concluded that for a QMF with magnetic field applied in the x direction, the effect of magnetic field on resolution enhancement is greater at higher ion energies because of increased Lorentz force.

Effect of an axial magnetic field on the performance of a QMF operating in zone 1

The effect of axial magnetic field on the mass spectrum is somewhat different compared with that of transverse, as there is reduction in low mass tail as well as high mass tail upon application of the magnetic field. Our previous work[30] described the effect of *Bz* on performance of a QMF in detail. With axial magnetic field, the mass filter can be operated close to the tip of stability zone 1. Figure 15 reproduced from[30] shows results for the effect of axial magnetic field on resolution and mass spectra. All the simulations used 99.99% as *U/V* ratio. Figure 15a shows the behavior of the resolution measured at 10% peak height as a function of axial magnetic field for three different lengths of QMF. For $L = 100$ mm, the resolution increases as *Bz* is varied between 0 and 0.035 T and then decreases as it is varied between 0.035 and 0.06 T, indicating that the QMF resolution will not increase indefinitely with *Bz*. This is because as *Bz* increases, the peak shape eventually degrades. A similar effect is seen for shorter and longer QMFs: resolution rises with applied *Bz* reaching a maximum value, then decreases. For the case of $L = 200$ mm, the predicted value of resolution is in excess of 3000 which if achieved in

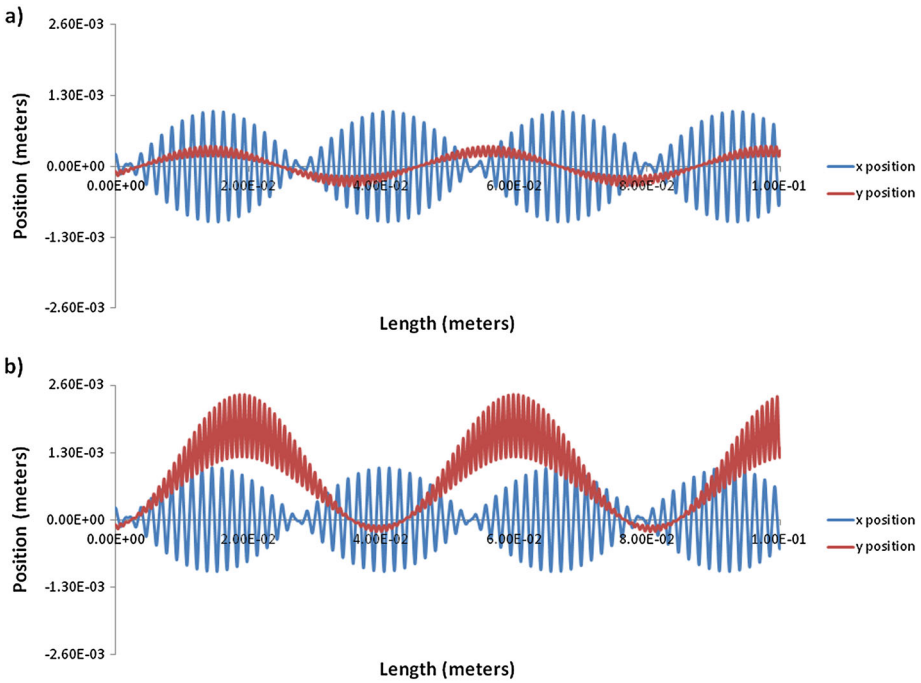

Figure 13. Numerical simulation of ion trajectories in x and y directions for $^{40}Ar^{+}$ with $Ez = 2$ eV and with (a) $B_x = 0$ T (upper trace) and (b) $B_x = 0.02$ T (lower trace).

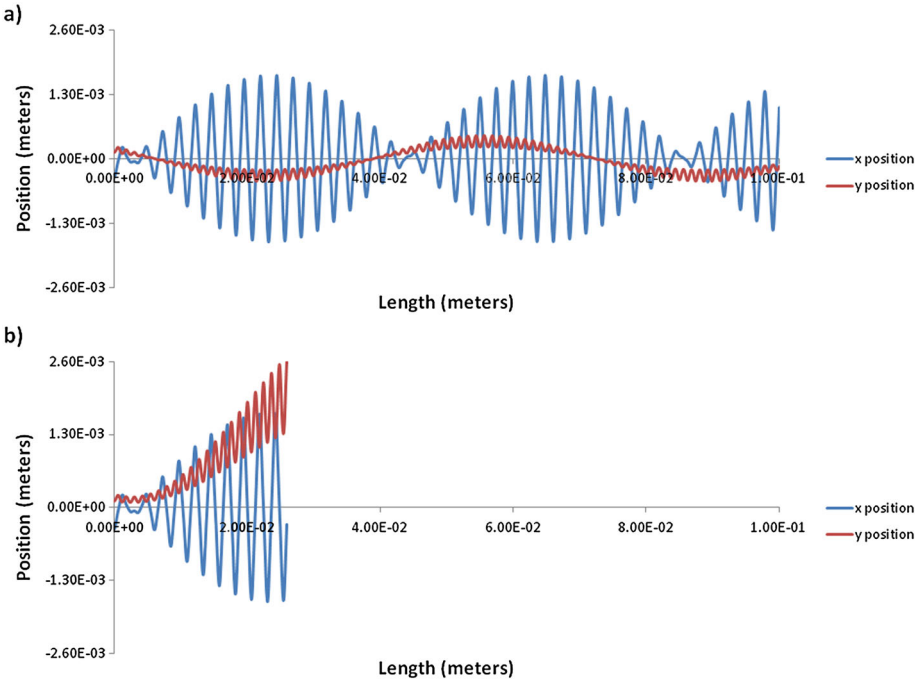

Figure 14. Numerical simulation of ion trajectories in *x* and *y* directions for $^{40}Ar^{+}$ with E_z = 5 eV and with (a) *Bx* = 0 (upper trace) and (b) *Bx* = 0.02 T (lower trace).

practice would allow specialist high resolution residual gas analysis (RGA) applications.

Figure 15b shows a set of $^{40}Ar^{+}$ mass spectral peaks for a hyperbolic QMF at different values of magnetic field (*Bz*) with electrode length *L* = 100 mm. An increase in resolution is clearly observed up to a magnetic field of 0.035 T. Transmission through the QMF decreases as magnetic field increases, which results in reduction of QMF resolution at higher values of magnetic field 0.045 – 0.06 T. A low-amplitude structure is present across the low mass and high mass sides of the mass peaks, due to minor changes in the acceptance of the QMF as the position of the mass scan changes. This is because the initial phase space positions of a large number of ions are very close to the QMF acceptance boundary, resulting in small local variations of transmission as the mass scan traverses the mass peak. This observed structure on the mass peak is an artifact of the simulation and can be reduced by increasing the number of ions although at the expense of increased simulation time.[30] Moreover, it was found that the effect of axial magnetic field is more pronounced as the number of rf cycles is increased.

Quadrupole mass spectrometer in the third stability zone with magnetic field applied

Simulation results

Effect of transverse magnetic field on the resolution of QMF operating at the upper tip of stability zone 3

The effect of transverse magnetic field on the performance of a QMF operating at the upper tip of stability region 3 has been described in detail previously. Figure 16, reproduced from[31] illustrates the effect of transverse magnetic field on the performance of a QMF operating at the upper tip of stability zone 3. Figure 16a shows the behavior of the resolution, measured at 10% peak height as a function of transverse magnetic field for two different values of *U/V* ratio, 104.81% (solid line) and 104.82% (dotted line). The details of the Mathieu stability zone 3 is shown in Figure 16c, where a *U/V* ratio of 100 % corresponds to *q* = 3.0 and *a* = 2.8 which is near the centre of the stability region. With increasing *U/V* ratio, the scan line approaches the upper left tip of stability zone 3, such that a *U/V* ratio of 104.82% corresponds to the scan line operating very close to the upper tip (*U/V* = 104.8315%) of the stability region. The resolution increases as *Bx* is varied between 0 and 0.0035 T; however, the QMF resolution will not increase indefinitely with *Bx*. This is because as *Bx* increases, the peak shape eventually degrades. In the case of *U/V* ratio = 104.82 %, the predicted value of resolution is in excess of 5000. This result shows that for any fixed value of *U/V* ratio, there is a resolution enhancement by simply applying transverse magnetic field to the body of the mass filter.

Figure 16b shows a set of simulated mass spectral peaks for $^{40}Ar^{+}$ from a hyperbolic QMF at different values of magnetic field applied in the *x* direction. An increase in resolution is clearly observed up to a magnetic field of 0.0035 T at the expense of reduction in number of ions transmitted. There is also a reduction in the low mass tail of the mass spectra with a magnetic field, a similar observation as zone 1.

Effect of axial magnetic field on the resolution of QMF operating at the upper tip of stability zone 3

Mass spectral studies of CO^{+} and N_2^{+} mixture

All the simulations are carried out in zone 3 and use 150 steps across the mass range, with 9×10^5 ion trajectories simulated at each point. Mass peaks for CO^{+} and N_2^{+} mixture are generated for a hyperbolic QMF with length (*L*) of 200 mm. The inscribed

Journal of MASS SPECTROMETRY

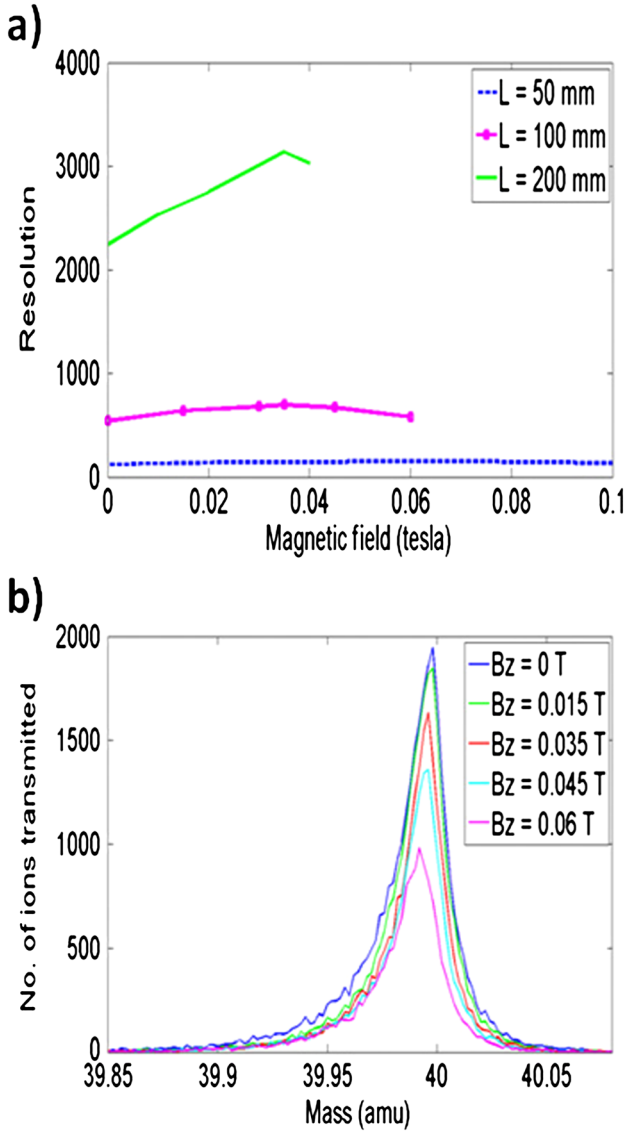

Figure 15. (a) The effect of magnetic field on resolution applied in the *z* direction (hyphenated *l* = 100 mm, dotted *l* = 50 mm, solid line *l* = 200). (b) Simulated mass peaks for $^{40}Ar^{+}$ with and without magnetic field for *l* = 100 mm.

radius of the QMF was taken to be 2.5 mm and the ion energy was chosen as 5 eV. The ion source radius (r_{ie}) was selected as 0.5 mm. The operating point (*U/V* ratio) was selected as 104.83%. The difference in mass between the two species is 0.0034 amu, requiring a minimum resolution of 8265 at 10% peak width definition for mass discrimination.

Figure 17a shows a set of peaks obtained with and without an applied axial magnetic field (B_z) for CO^+ and N_2^+ mixture within a hyperbolic QMF at a frequency of 5 MHz. An increase in resolution is clearly observed with an applied magnetic field of 0.001 T, howbeit at the expense of sensitivity. Figure 17b shows a set of peaks obtained with and without an applied magnetic field of 0.00075 T for CO^+ and N_2^+ mixture at a frequency of 8 MHz. From Fig. 17a, it can be seen that there is a clear improvement in resolution at 10% peak height with magnetic field applied, from approximately R = 13 338 to R = 15 562 (~16.7% increase) for the CO^+ and N_2^+ mixture. Whereas, from Fig. 17b, it can be seen that upon application of magnetic field, the resolution increases approximately from, R = 21 546 to R = 26 676 (~23.8% increase). Moreover, it should be noted that a lower value of magnetic field was required at higher frequency to increase the resolution; this effect is explained later in the paper. The obtained resolutions are far higher than the minimum resolution required to separate the two species; this simulation result clearly illustrates the resolution enhancement provided by axial magnetic field in stability zone 3.

The effect of magnetic field in the z direction on the resolution of QMF

The simulated mass peaks for $^{40}Ar^{+}$ ions using the computer software are shown in Fig. 18. All the simulations used 150 steps across the mass range, with 9×10^5 ion trajectories simulated at each point. Mass peaks for $^{40}Ar^{+}$ are generated for a hyperbolic QMF with length (*L*) of 100 mm. The inscribed radius of the QMF was taken to be 1.5 mm. The frequency of the rf voltage used in the simulation was 5 MHz and the ion energy was chosen as 5 eV. The ion source radius (r_{ie}) was selected as 0.5 mm and the exit radius was chosen as 3 mm. The operating point (*U/V* ratio) was selected as 104.82%. Figure 18a shows the behavior of the resolution (measured at 10% peak height) as a function of axial magnetic field; the resolution increases as *Bz* is varied between 0 and 0.002 T and then decreases as it is varied between 0.002 and 0.0075 T.

Figure 18b shows a set of $^{40}Ar^{+}$ mass spectral peaks for a hyperbolic QMF at different values of magnetic field (*Bz*). An increase in resolution is clearly observed up to a magnetic field of 0.002 T. Transmission through the QMF decreases as magnetic field increases, which results in reduction of QMF resolution at higher values of magnetic field 0.003 – 0.0075 T. A shift in mass peak is observed at higher values of magnetic field. Even with B = 0, this is a common feature observed for a QMF operating in stability zone 3.

The effect of magnetic field in the z direction on ion trajectories

Figure 19 shows typical behavior of the ion trajectories calculated using the theoretical model for ions transmitted with and without the axial magnetic field applied. All the simulations were carried out in stability zone 3. The corresponding traces shown in the figure are for the same ion injected into the mass filter at the same point in time (rf phase) and space and at the same point on the mass scale (m = 40.00 amu). The upper trace of the figure is for the case with no field applied and lower trace with B_z of 0.0015 T.

Ion motion in Fig. 19 originates at $x = -1.78 \times 10^{-4}$ m and $y = 1.64 \times 10^{-6}$ m with initial velocity of 4.90×10^3 m/s. In the lower trace, due to the additional magnetic component of the Lorentz force provided by B_z, the amplitude of ion trajectory along the *y* direction increases. The application of magnetic field therefore displaces the ion in the *y* direction so that the ion is lost through impact with the electrodes (r_0 = 1.5 mm).

The effect of ion energy on resolution in the presence of magnetic field in the z direction

Figure 20 shows the dependence of resolution on ion energy for $^{40}Ar^{+}$ with and without magnetic field applied. As can be seen from Fig. 20, in both cases, resolution decreases with increase in ion energy. However, it can also be observed that percentage increase in resolution with magnetic field decreases as ion energy increases. It should also be noted that in the presence of magnetic field of same intensity the resolution is poorer at

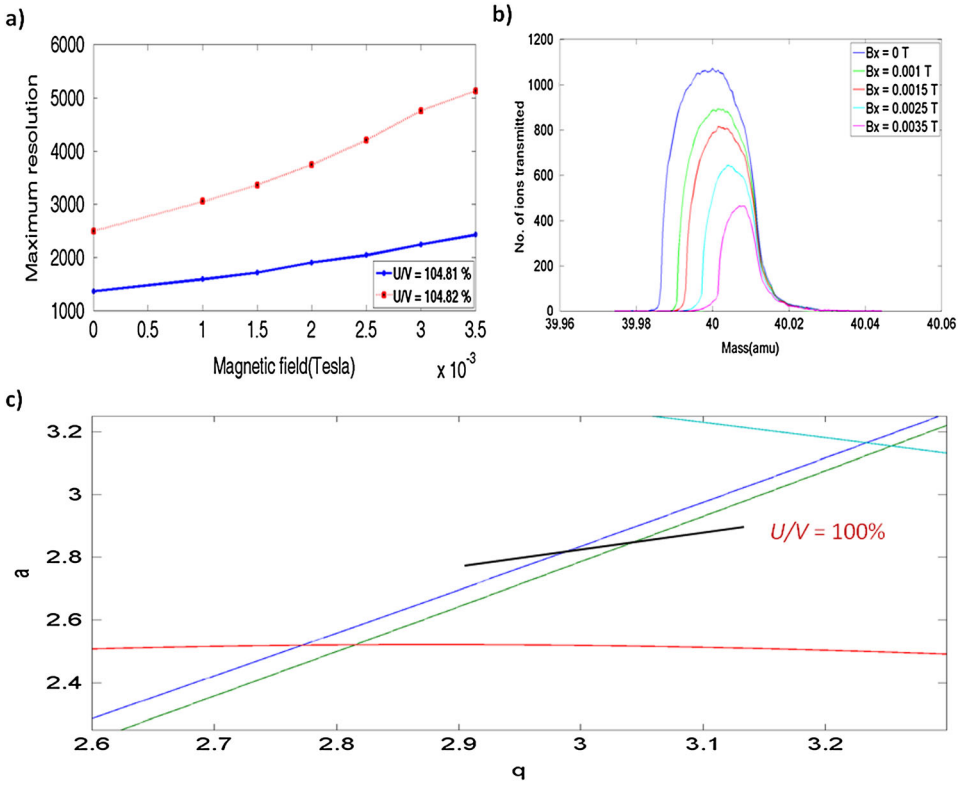

Figure 16. (a) The effect of magnetic field on resolution of $^{40}Ar^{+}$ applied in the *x* direction (solid line (*U/V* = 108.81%) and dotted line (*U/V* = 104.82 %); the zone 3 detail of the Mathieu stability diagram is shown in the inset. (b) Simulated mass peaks for $^{40}Ar^{+}$ with and without magnetic field. (c) a-q diagram of the upper stability region for QMS operation showing the U/V scan line.

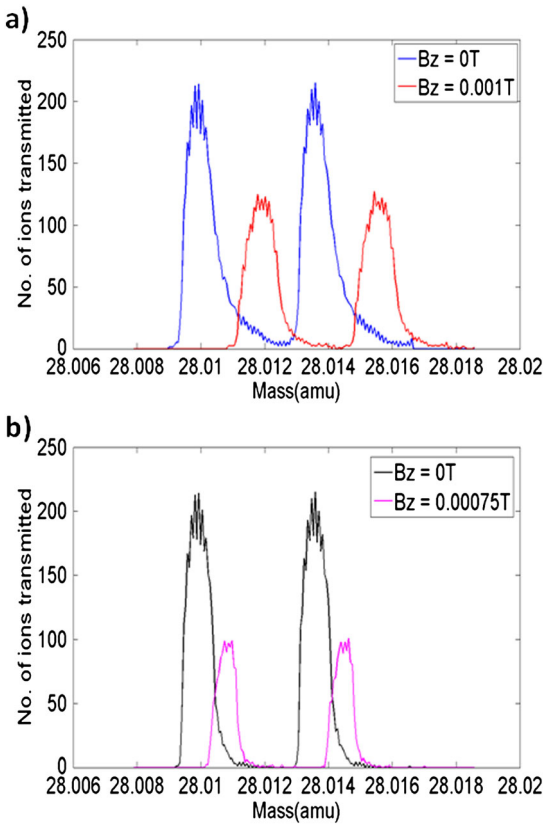

Figure 17. (a) Simulated mass peaks for CO^{+} and N_2^{+} mixture with and without magnetic field applied (B_x = 0.001 T), frequency 5 MHz. (b) Simulated mass peaks for CO^{+} and N_2^{+} with and without magnetic field applied (B_x = 0.00075 T), frequency 8 MHz.

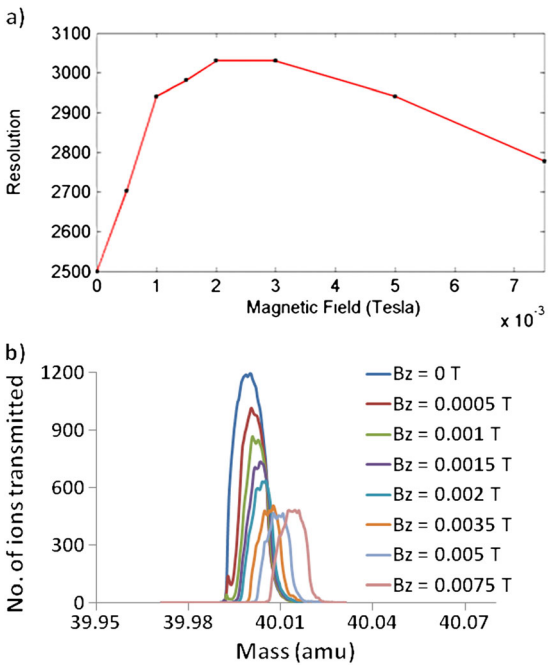

Figure 18. (a) The effect of magnetic field on resolution applied in *z* direction. (b) Simulated mass peaks for $^{40}Ar^{+}$ with and without magnetic field.

Ez = 20 eV (compared with B = 0). This effect is attributed to the fact that in the presence of axial magnetic field the percentage increase in resolution is higher for a larger number of rf cycles (a similar case is observed for zone 1

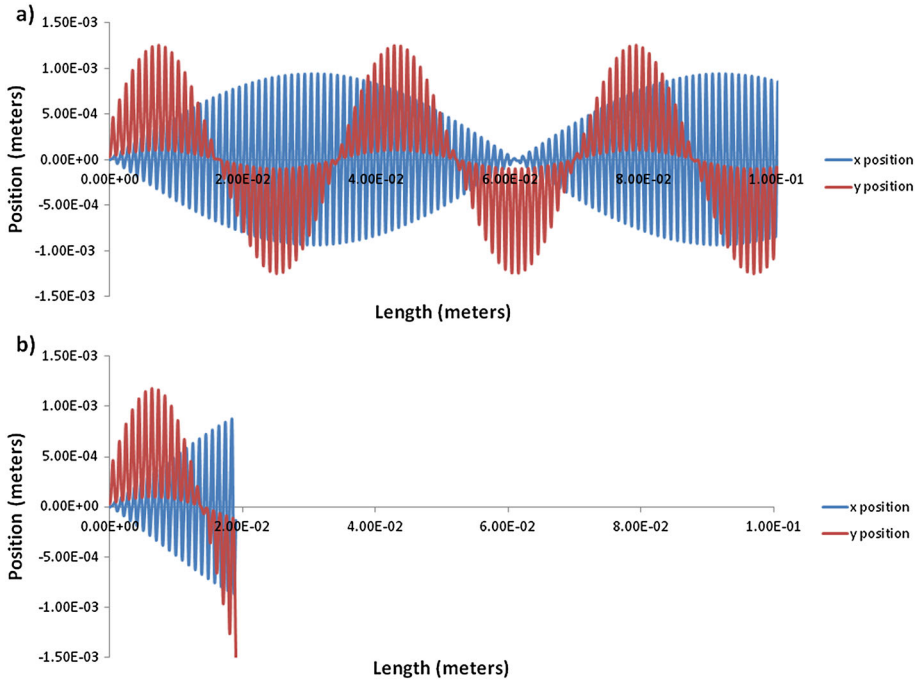

Figure 19. Numerical simulation of ion trajectories in *x* and *y* directions for $^{40}Ar^{+}$ with (a) *Bz* = 0 (upper trace) and (b) *Bz* = 0.0015 T (lower trace).

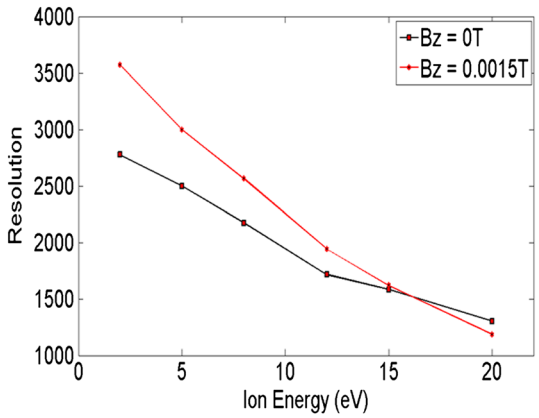

Figure 20. The dependence of resolution on ion energy with and without an applied magnetic field.

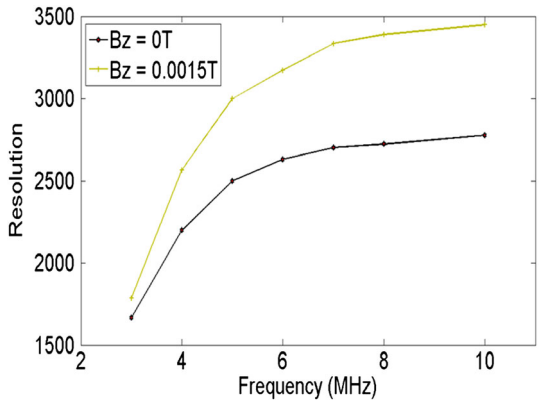

Figure 22. The dependence of resolution on frequency with and without an applied magnetic field.

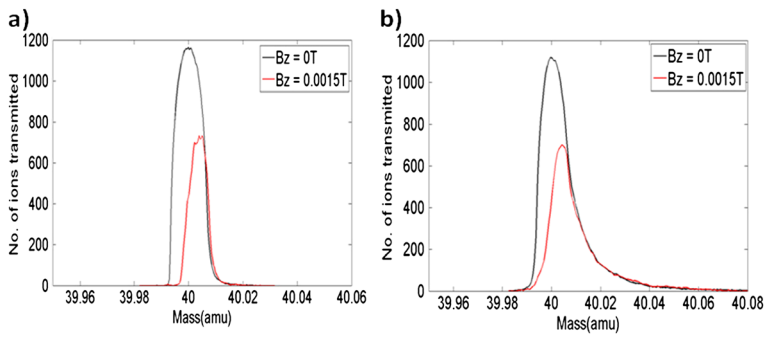

Figure 21. Mass peaks for $^{40}Ar^{+}$ with and without an axial magnetic field applied. (a) for Ez = 2 eV. (b) for Ez = 20 eV.

operation). Moreover, the behavior of the peak shape for stability zone 3 contributes to this effect. Figure 21a shows mass peaks for $^{40}Ar^{+}$ with and without an axial magnetic field applied of *Bz* = 0.0015 T for Ez = 2 eV. Whereas, Fig. 21b shows mass peaks for $^{40}Ar^{+}$ with and without an axial magnetic field applied of *Bz* = 0.0015 T for *Ez* = 20 eV.

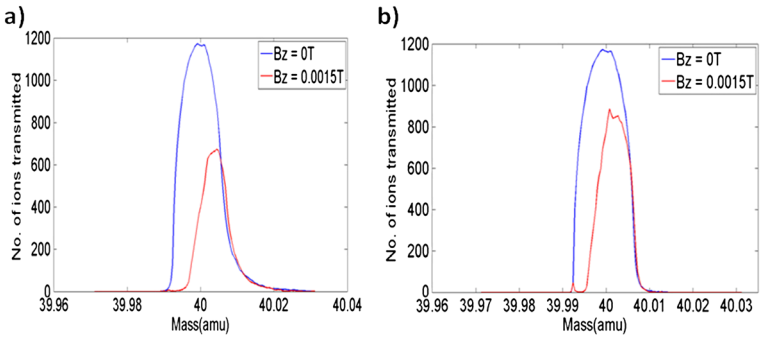

Figure 23. Mass peaks for $^{40}Ar^{+}$ with and without an axial magnetic field applied. (a) for f = 4 MHz; (b) for f = 8 MHz.

As seen from Fig. 21a at low values of ion energy (i.e. large number of rf cycles), the shape of the mass peaks predicted are high quality with very low amplitude of high mass tail, which is a common feature of mass peaks obtained for a QMF operated in zone 3. Figure 21b shows mass peaks at a high value of ion energy (i.e. low number of rf cycles); the shape of the mass speak is poor as the amplitude of the high mass tail is very high.

The effect of frequency on resolution in the presence of magnetic field in the z direction

Figure 22 shows the dependence of resolution on frequency for $^{40}Ar^{+}$ with and without magnetic field applied. As can be seen from Fig. 22, in both cases, resolution increases with increase in frequency. For the case Bz = 0 T, resolution increases with increase in frequency because the number of rf cycles increases[14]; and the resolution enhancement will eventually saturate as the number of rf cycles is increased as explained in.[34] A similar trend is observed with Bz applied. However, it can also be observed that percentage increase in resolution with applied magnetic field increases as frequency increases. This effect has been observed previously where the percentage increase in resolution is higher for a larger number of rf cycles with axial magnetic field applied.[30] Moreover, as discussed in the previous subsection, the behavior of the peak shapes for stability zone 3 contributes to this effect. Figure 23a shows mass peaks for $^{40}Ar^{+}$ with and without an axial magnetic field applied (Bz = 0.0015 T, f = 4 MHz). Whereas, Fig. 23b shows mass peaks for $^{40}Ar^{+}$ with and without an axial magnetic field applied (Bz = 0.0015 T, f = 8 MHz).

As seen from Fig. 23a at low values of frequency (i.e. low number of rf cycles), the shape of the mass peak is poor as the amplitude of high mass tail is high. This contributes to small increase or a decrease in resolution depending on the value of magnetic field, due to the peak degradation as sensitivity decreases and also due to the presence of an increased amplitude high mass tail. Figure 23b shows mass peaks at a high value of frequency (i.e. large number of rf cycles); high quality peak shapes (low tailing of the peak) give an increase in resolution with the magnetic field applied (resolution measured at 10% peak height).

Conclusions

In this work, experimental results are presented for a QMS instrument showing an increase in resolution when a static magnetic field is applied along the mass filter length for operation in stability zone 1. The resolution enhancement observed experimentally has been simulated theoretically using custom software developed at the University of Liverpool. The model predicts an ultimate increase in resolution which cannot be achieved by adjustment of the U/V ratio alone. The effects may be explained by considering the fact that, in the presence of a static magnetic field in addition to the alternating quadrupole field, an ion experiences an additional magnetic component of Lorentz force which modifies its motion. This results in rejection of ions in the low mass tail and/or high mass tail depending on the orientation of the magnetic field vector giving reduced peak widths for a set of operating conditions. A comprehensive simulation study has been carried out to show the effects of different input parameters such as variation of ion energy and drive frequency under the influence of magnetic field. As a result of applying magnetic field, high resolutions (R > 3000) are predicted for a QMF of length 200 mm operating in stability zone 1 allowing wider instrument application.

Simulation studies have been carried out using the software to show the possibilities of achieving enhanced resolution under the influence of static magnetic field applied in both ***axial*** and ***transverse*** directions for QMF operation in stability zone 3. For a QMF of length 200 mm, the model predicts instrument resolution R>26 000 for a CO_2 and N_2 mixture via application of an axial magnetic field. These features suggest wider applications than hitherto for such QMS instruments (e.g. applications in which extremely high QMS resolution and/or high abundance sensitivity are required). These include identification of gaseous species with nominally overlapping mass peaks for conventional QMS.

Future work will endeavor to investigate the effect of the magnetic field experimentally on the QMS instrument operating in stability zone 3. Furthermore, experimental results obtained hitherto have been for a relatively low-resolution QMS and verification of performance enhancement for a high-resolution instrument is necessary.

References

[1] J. J. Thomson. Rays of positive electricity and their application to chemical analyses, Longmans green and co. 1913, **1921**.
[2] F. W. Aston. Isotopes, Arnold, London. **1922**.
[3] A. J. Dempster. A new method of positive ray analysis. *Phys. Rev.* **1918**, *11(4)*, 316–325.
[4] S. Borman, H. Russell, G. Siuzdak. Mass spec timeline. *Chem. chronicles* **2003**, 47–49.
[5] A. O. Nier. A double-Focusing Mass Spectrometer. *Nat. Bur. Stand. Circ. (U.S.)*. **1953**, *522*, 29–36.
[6] W. C. Wiley, I. H. McLaren. Time-of-flight mass spectrometer with improved resolution. *Rev. Sci. Instrum.* **1955**, *26*, 1150–1157,
[7] W. Paul, H. P. Reinhard, Z. U. Von. Das elektrische massenfilter asl massenspektrometer and isotopentrenner. *Z Phys.* **1958**, *152*, 143–182.

[8] M. B. Cumisarow, A. G. Marshall. Fourier transform ion cyclotron resonance spectroscopy. *Chem. Phys. Lett.* **1974**, *25*(2), 282–283,
[9] W. Paul, M. Raether. Das elektrische massenfilter. *Zeitschrift fur Physik.* **1955**. *40*, 262–273.
[10] D. J. Douglas. Linear quadrupoles in mass spectrometry. *Mass Spectrom. Rev.* **2009**, *28*, 937–960.
[11] U. Von Zahn. Prazisions-massenbestimmungen mit dem elekrischen massenfilter. *Zeitschrift fur Physik* **1962**, *168*, 129–142.
[12] W. M. Brubaker, J. Tuul. Performance studies of a quadrupole mass filter. *Rev. Sci. Instrum.* **1964**, *35*(8), 1007–1010.
[13] A. E. Holme, W. J. Thatcher, J. H. Leck. An investigation of the factors determining maximum resolution in a quadrupole mass spectrometer. *J. Phys. E Sci. Instrum.* **1972**, *5*, 429–433.
[14] P. H. Dawson. Quadrupole mass spectrometry and its applications, Elsevier: Amsterdam, **1976**.
[15] J. H. Batey. Quadrupole gas analyzers. *Vacuum* **1987**, *37*, 659–668.
[16] N. V. Konenkov. Influence of fringing fields on the acceptance of a quadrupole mass filter in the separation mode of the intermediate stability region. *Int. J. Mass. Spectrom. Ion Process.* **1993**, *123*, 101–105.
[17] C. Trajber, M. Simon, S. Bohatka, I. Futo. A mass independent prefilter arrangement for quadrupole mass spectrometer. *Vacuum* **1993**, *44*(4-7), 653–656.
[18] F. Muntean. Transmission study for r.f – only quadrupoles by computer simulations. *Int. J. Mass. Spectrom. Ion Process.* **1995**, *151*, 197–206.
[19] J. J. Tunstall, A. C. C. Voo, S. Taylor. Computer simulation of the mass filter for a finite length quadrupole. *Rapid Commun. Mass Spectrom.* **1997**, *11*, 184–188.
[20] J. R. Gibson, S. Taylor, J. H. Leck. Detailed simulation of mass spectra for quadrupole mass spectrometer systems. *J. Vac. Sci. Technol. A.* **2000**, *18*(1), 237–243.
[21] J. R. Gibson, S. Taylor. Prediction of quadrupole mass filter performance for hyperbolic and circular cross section electrodes. *Rapid Commun. Mass Spectrom.* **2000**, *14*, 1669–1673.
[22] Z. Du, D. J. Douglas, T. Glebova, N. V. Konenkov. Peak structure with a quadrupole mass filter operated in the third stability region. *Int. J. Mass. Spectrom.* **2000**, *197*, 113–121.
[23] D. J. Douglas, T. A. Glebova, N. V. Konenkov, M. Y. Sudakov. Spatial harmonics of the field in a quadrupole mass filter with circular electrodes. *Tech. Phys.* **1991**, *44*(10), 1215–1219.
[24] J. Sreekumar, T. J. Hogan, S. Taylor, P. Turner, C. A. Knott. Quadrupole Mass Spectrometer for Resolution of Low Mass Isotopes. *J. Am. Soc. Mass Spectrom.* **2010**.
[25] J. R. Ahn, C. J. Park. Computer simulations of electron and ion trajectories in electron-impact ion sources of a quadrupole mass spectrometer. *Nucl. Instrum. Meth. Phys. Res. A* **2011**, *645*, 345–349.
[26] J. K. Gooden, D. L. Rempel, M. L. Gross. Evaluation of Different Combinations of Gated Trapping, RF-Only Mode and Trap Compensation for In-Field MALDI Fourier Transform Mass Spectrometry. *J. Am. Soc. Mass Spectrom.* **2004**, *15*, 1109–1115.
[27] D. M. Desiderio, N. M. Nibbering. Mass Spectrometry: Instrumentation, Interpretation, and Applications. Wiley, New Jersey, **2008**.
[28] J. J. Tunstall, S. Taylor, A. Vourdas, J. H. Leck, J. Batey. Application of static magnetic field to the mass filter of a quadrupole mass spectrometer. *Vacuum* **1999**, *53*, 211–213.
[29] B. Srigengan, J. R. Gibson, S. Taylor. Ion trajectories in quadrupole mass spectrometer with a static transverse magnetic field applied to mass filter. *IEE Proc-Sci. Meas. Technol.* **2000**, *147*(6), 274–278.
[30] S. U. A. H. Syed, J. Sreekumar, B. Brkic, J. R. Gibson, S. Taylor. Effect of an axial magnetic field on the performance of a Quadrupole Mass Spectrometer. *J. Am. Soc. Mass Spectrom.* **2010**, *21*, 2070–2076.
[31] S. U. A. H. Syed, J. Sreekumar, J. R. Gibson, S. Taylor. QMS in the third stability zone with a transverse magnetic field applied. *J. Am. Soc. Mass Spectrom.* **2011**, *22*, 1381–1387.
[32] R. P. Feynman, M. Sands. The Feynman lectures on Physics, Vol (2), Addison Wesley: Reading, Massachusetts, **1977**.
[33] S. Maher, S. U. A. H. Syed, D. M. Hughes, J. R. Gibson, S. Taylor. Mapping the stability diagram of a quadrupole mass spectrometer with a static transverse magnetic field applied. *J. Am. Soc. Mass Spectrom.* **2013**, *24*(8), 1307–1314.
[34] S. U. Syed, T. J. Hogan, M. J. Joseph, S. Maher, S. Taylor. Quadrupole mass filter: design and performance for operation in stability zone 3. *J. Am. Soc. Mass Spectrom.* **2013**, *24*(10), 1493–1500.

